Supporting Information

Facet control of manganese oxides with diverse redox abilities and acidities for catalytic removing the hazardous 1,2-dichloroethane

Baicheng Shi[1], Zhaoying Di, Xiaonan Guo, Ying Wei, Runduo Zhang*, Jingbo Jia*

State Key Laboratory of Chemical Resource Engineering, Beijing Key Laboratory of Energy and Environmental Catalysis, Beijing University of Chemical Technology, Beijing 100029, P. R. China

*corresponding author: R. Zhang (zhangrd@mail.buct.edu.cn)
J. Jia (jiajb@mail.buct.edu.cn)

S1. Preparation

α-MnO_2: 1.35 g of $KMnO_4$ and 3.0 mL of HCl (37 wt%) were added to deionized water. After stirring for 30 min, the solution was transferred to a Teflon-lined stainless-steel autoclave, sealed, and maintained at 120 °C for 12 h in an electric oven.

β-MnO_2: The mixture of 1.69 g $MnSO_4$ and 2.28 g $(NH_4)_2S_2O_8$ was added to deionized water with stirring for 30 min. Then, the solution was transferred to a Teflon-lined stainless-steel autoclave, sealed, and maintained at 140°C for 12 h.

γ-MnO_2: The mixture of 6.32 g $MnSO_4$ and 8.56 g $(NH_4)_2S_2O_8$ was added to deionized water. After stirring for about 30 min, the solution was transferred to a Teflon-lined stainless-steel autoclave, sealed, and maintained at 90°C for 24 h in oven.

δ-MnO_2: 1.35 g of $KMnO_4$ and 1.0 mL of HCl (37 wt%) were added to deionized water, After stirring magnetically for about 30 min, the solution was transferred to a Teflon-lined stainless-steel autoclave and crystallized at 100°C for 12 h.

After the hydrothermal reaction, the autoclave was cooled to room temperature. The sediment was centrifuged, washed with distilled water and ethanol several times, dried at 80°C for 12 h, and then calcined at 300°C for 8 h to obtain the corresponding samples.

S2. Characterization

The crystallographic information of sample was investigated by X-ray diffraction using a diffractometer equipped with Cu *Kα* radiation (λ = 0.15406 nm, D8FOCUS, Bruker). Diffractograms were collected in the 2θ range between 10^o and 80^o by step of 0.1^o. Phase identification was made by a comparison with JCPDS database.

The information of specific surface area (S_{BET}) was collected by N_2 sorption isotherm using a Quanta chrome Autosorb IQ analyzer at liquid N_2 temperature (-196 ^{o}C). Before analysis, samples were outgassed at 300 °C under vacuum for 10 h. Brunauer-Emmett-Teller (BET) surface area was calculated using experimental points at a relative pressure of P/P_0 = 0.05~0.35.

H_2-TPR experiment was carried out in a chemisorption device. Prior to the measurement, the samples were degassed under flowing nitrogen (30 ml/min) at 300 ^{o}C for 1 h. After cooling in nitrogen to 100 ^{o}C, a 5% H_2/N_2 flow of 30 ml/min was introduced to pass through a quartz reactor containing the sample (100 mg). The consumption of H_2 along with heating temperature was online recorded by a thermal conductivity detector (TCD, Huasi, China) and the signals of TCD were collected

from 100°C to 600°C in nitrogen flow.

Temperature-programmed desorption of O_2 (O_2-TPD) was also analyzed with an online mass spectrometer. The concentrations of O_2 and CO_2 were determined using m/z=32 and m/z=44, respectively. For the O_2-TPD, 0.1 g of catalyst was pretreated at 200 °C with Ar for 30 min, and then 10% O_2/Ar was introduced on the surface of the catalyst for 60 min at 100 °C. Next, the sample was purged with Ar for 1 h to remove the exterior adsorbed molecular oxygen and the catalyst was cooled down to ambient temperature, Finally, the microreactor was heated from ambient temperature to 650 °C with a heating rate of 5 °C·min^{-1} under Ar flow.

The NH_3 temperature programmed desorption (NH_3-TPD) experiment was taken on a device with a thermal conductivity detector (TCD, Huasi, China). The sample (100 mg) was first pretreated at 300°C under nitrogen flow for 0.5 hr. After cooling to 100°C, the sample was saturated in 10% NH_3/N_2 atmosphere for 1 h and then exposed in nitrogen atmosphere for 0.5 h to eliminate the influence of physisorbed NH_3. Finally, the signals of TCD were collected from 100°C to 600°C in nitrogen flow.

A S-4800 (Hitachi, Japan) scanning electron microscope (SEM) was employed to characterize the morphology of the prepared MnO_2 solids (the accelerating voltage is 5.0 kV). The powders were coated onto a conductive tape. Besides, a JEM-2100 (Jeol, Japan) high-resolution transmission electron microscopy (HRTEM) was also employed to observe the crystal lattice fringe and internal microstructure (the operating voltage is 200 kV).

X-ray photoelectron spectroscopy (XPS) instrument (Shimadzu, Japan) equipped with a monochromatic Mg/Al Kα was used to analyze the superficial layer properties. The binding energy was calibrated by the C 1s peak (B.E.=284.8eV) as a reference. The surface composition and chemical state were determined according to the position and areas of binding energies of Mn 2p, Mn 3s and O 1s peaks.

The *in situ* DRIFTS experiments were performed using an infrared spectrometer (TENSOR 27, BRUKER) that was configured with liquid N_2-cooled highly sensitive mercury cadmium telluride (MCT) detector. The reaction chamber (Praying Mantis, Harrick) as a diffuse reflection accessory included a diffuse reflectance cell (Harrick) with CaF_2 windows and a heating cartridge that could control the desired temperatures. Before the test, about 50mg finely ground samples were padding in the in situ

chamber and heated under flowing Ar at 300 ℃ for 1 h to remove water from the surface and pores of the catalyst, the samples were then cooled to 50℃ in Ar atmosphere. After that, the gaseous mixture of Ar + O_2 +1, 2-DCE with a flow rate of 40 mL/min and 400 ppm 1, 2-DCE, 20% O_2 in Ar was introduced into the chamber. The spectra were collected in 64 scans at a resolution of 4 cm^{-1} within 850–3800 cm^{-1}. The sample was tested in the range of 50–300 °C.

S3. Temperature-programmed oxygen isotopic exchange (OIE) reaction

This experiment is performed on an oxygen isotope device, which includes a vacuum pump, a circulation pump, a heating furnace, an U-shaped micro-reaction tube (V = 70 cm^3), and many gas pipelines, the signals of reactants were recorded by mass spectrometer (OmniStar, Germany). The sample (100 mg) was pretreated in O_2 atmosphere by heating to 300°C. When the temperature dropped to 200°C, redundant $^{16}O_2$ was removed under the condition of dynamic vacuum for 30 min. Then, 65.0 ± 1.5 mbar of pure Oxygen isotopic ($^{18}O_2$) was introduced into the reaction system for OIE reaction, and the catalyst was heated to 600°C and the mass spectrometer is turned on at the same time. The concentration changes of $^{18}O_2$ (P36), $^{16}O_2$ (P32), and $^{16}O^{18}O$ (P34) during the oxygen exchange reaction were recorded by mass spectrometer. Besides, N_2 (m/z=28) was also recorded in order to detect possible vacuum system leaks. Figure S1 shows a schematic diagram of an oxygen isotopic exchange device.

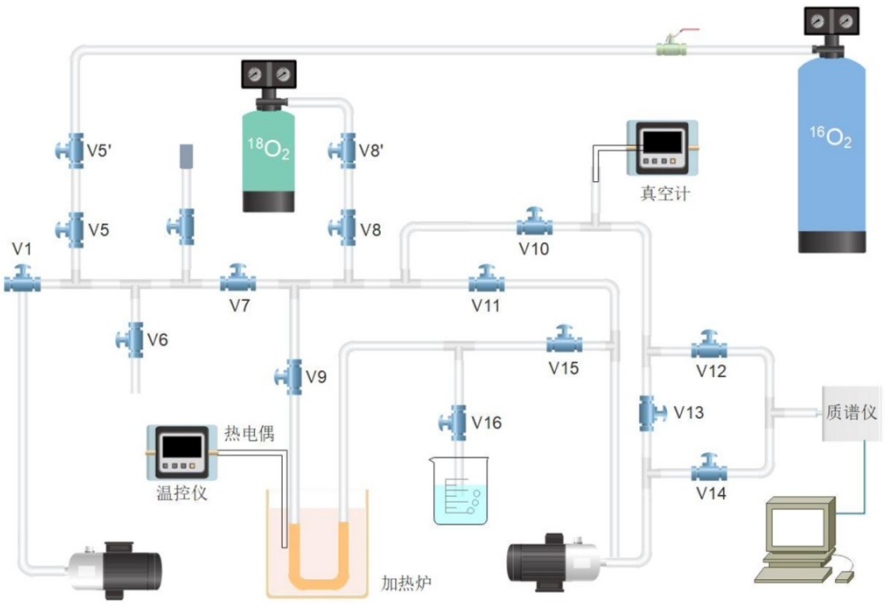

Figure S1: Schematic diagram of the oxygen isotopic exchange experiment

S4. Computational details

Spin-polarized Periodic Density Functional Theory (DFT) calculations were accomplished with the Vienna simulation package VASP [S1]. The projector augmented plane wave (PAW) approach [S2-S3] was applied to the electron-ion interaction together with generalized gradient GGA-PW91 [S4].

S5. Catalytic activity and products yield

The following equations were used to calculate the conversion of 1,2-DCE as well as the CO, CO_2 and HCl yields :

$$1{,}2-DCE\ conversion\ (\%) = \frac{[1{,}2-DCE]_{in} - [1{,}2-DCE]_{out}}{[1{,}2-DCE]_{in}} \times 100 \quad (1)$$

$$CO\ yield\ (\%) = \frac{[CO]}{[CO] + [CO_2] + x[C_xH_yCl_z]} \times 1{,}2-DCE\ conversion \times 100 \quad (2)$$

$$CO_2\ yield\ (\%) = \frac{[CO_2]}{[CO] + [CO_2] + x[C_xH_yCl_z]} \times 1{,}2-DCE\ conversion \times 100 \quad (3)$$

$$HCl\ yield\ (\%) = \frac{[HCl]}{[HCl] + 2[Cl_2] + z[C_xH_yCl_z]} \times 1{,}2-DCE\ conversion \times 100 \quad (4)$$

$$C_xH_yCl_z\ yield\ (\%) = \frac{x[C_xH_yCl_z]}{[CO] + [CO_2] + x[C_xH_yCl_z]} \times 1{,}2-DCE\ conversion \times 100 \quad (5)$$

S6. Byproducts of catalyst combustion

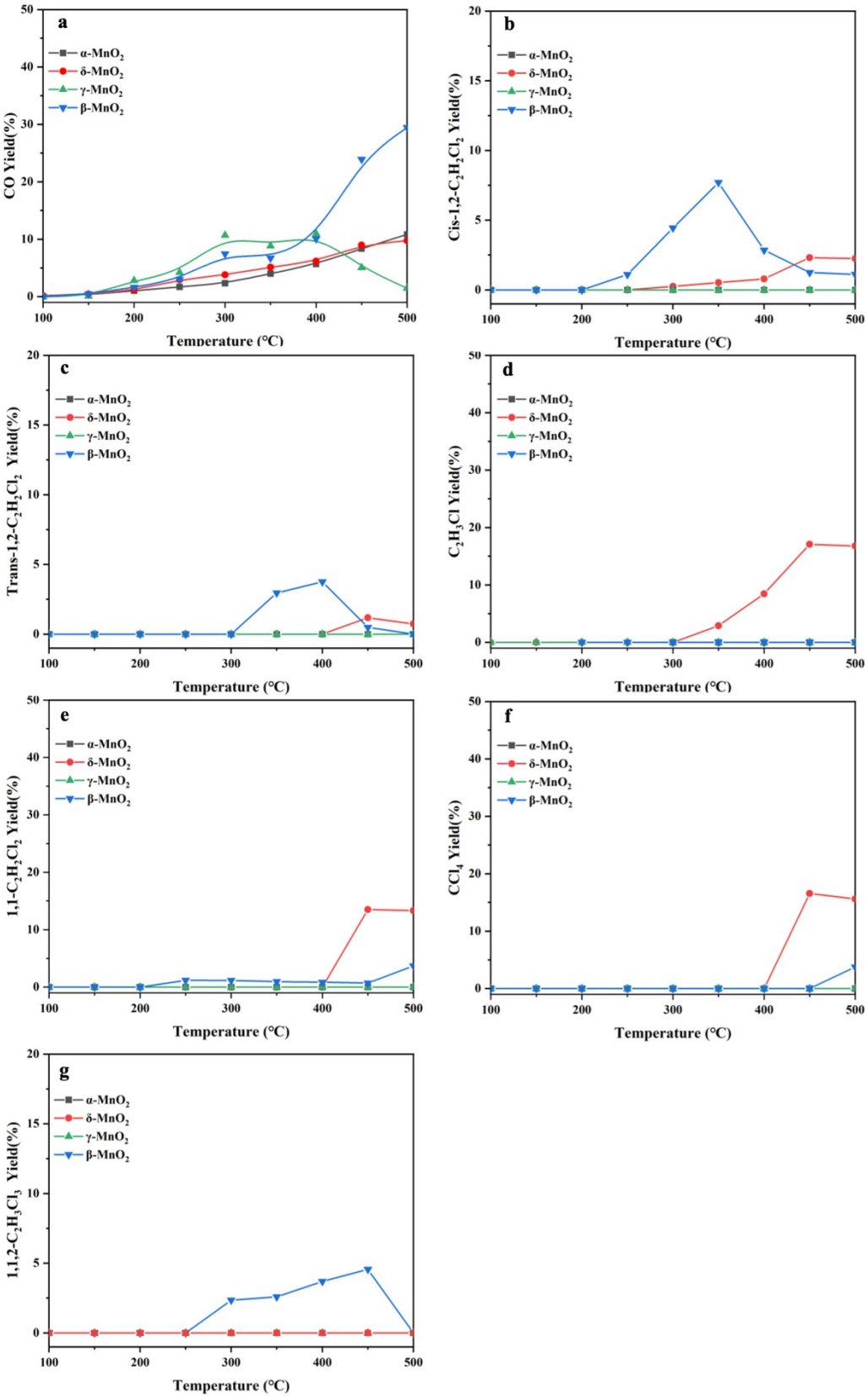

Figure S2: Yields of (a) CO, (b) cis-1,2-$C_2H_2Cl_2$, (c) trans-1,2-$C_2H_2Cl_2$, (d) C_2H_3Cl, (e) 1,1-$C_2H_2Cl_2$, (f) CCl_4 and (g) 1,1,2-$C_2H_3Cl_3$ over α-, β-, γ- and δ-MnO_2 samples.

Figure S2 shows the byproduct yields of 1,2-dichloroethane (1,2-DCE) combustion

over α-, β-, γ- and δ-MnO_2 samples. α-MnO_2 presents a gradual increasing trend for CO yield, and cannot observe a decreasing trend. β-MnO_2 exhibits the highest CO yield, owing to the poor redox ability. γ-MnO_2 shows a trend of increasing first and then decreasing, which means CO can be further oxidized at high temperatures. Similar to the α-MnO_2, δ-MnO_2 also displays the same trend because of the production of too many chlorined byproducts, which hinders CO further transformation. No obvious chlorined byproducts are found on α- and γ-MnO_2, but there are many chlorined byproducts are found on β- and δ-MnO_2, especially on δ-MnO_2. Vinyl chloride (C_2H_3Cl) (Fig. S2 d) is produced due to the removal of 1,2-DCE by HCl elimination at 300°C. Then at 400 °C, an electrophilic substitution reaction between HCl and vinyl chloride was followed to form cis-dichloroethylene and trans-dichloroethylene (cis-1,2-$C_2H_2Cl_2$ and trans-1,2-$C_2H_2Cl_2$) (Fig. S2 b and c), some of which also become 1,1-dichloroethene (1,1-$C_2H_2Cl_2$) (Fig. S2 e), part of 1,2-DCE breaks the C-H and C-C bond, gradually becomes CCl_4 (Fig. S2 i) , and this part of the polychlorinated byproducts was formed at last without further transformation, the results show that the yield of HCl at high temperature (> 400°C) was very low. Similar to δ-MnO_2, the overall yield of HCl from β-MnO_2 was also low, and several reaction products (such as *cis*-1,2-dichloroethene, *trans*-1,2-dichloroethene, 1,1-dichloroetheneand and tetrachloromethane) are found to be identical to δ-MnO_2. Notably, the presence of 1,1,2-trichloroethane (1,1,2-$C_2H_3Cl_3$) (Fig. S2 g) was noticed on the β-MnO_2, indicating that the dehydrochlorination and chlorination of vinyl chloride might take place.

S7. Cl mass balance of all these products

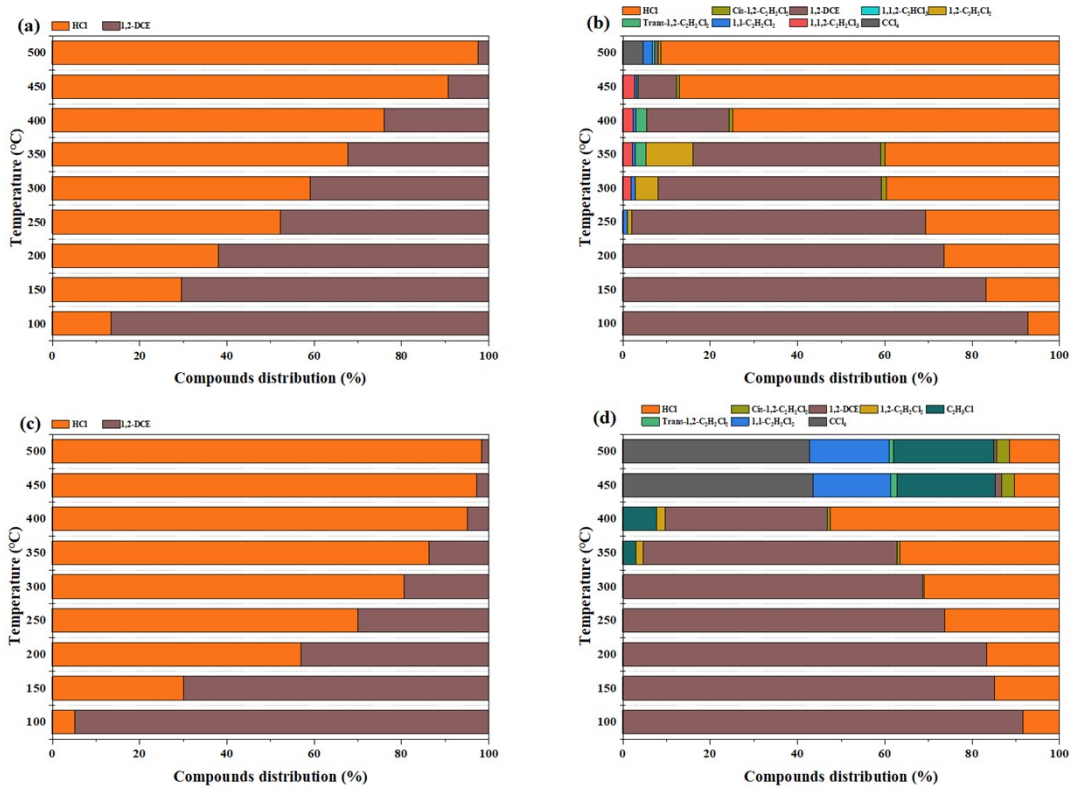

Figure S3. The chlorine mass balance during the 1, 2-DEC oxidation over (a) α-, (b) β-, (c) γ- and (d) δ-MnO_2

It can be found that the sum of the yields of different detected Cl-containing substances is close to 100% (Figure S3).

S8. Catalystic stability test

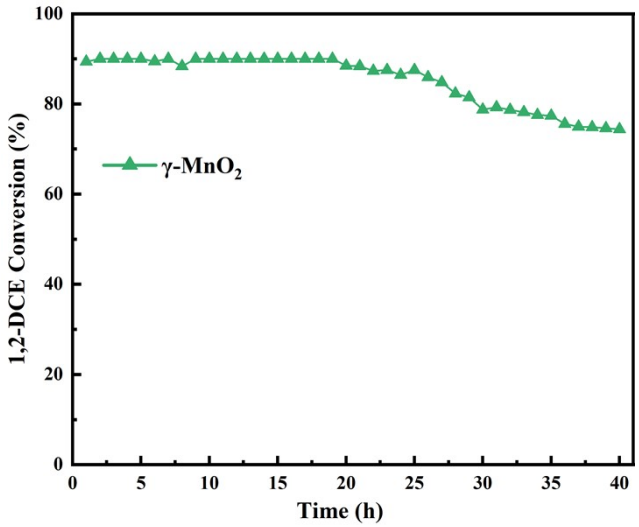

Fig. S4. Stability test of γ-MnO_2

The stability of the best-performing γ-MnO_2 catalyst is investigated as shown in **Fig. S4**. This catalyst was tested for1, 2-DCE oxidation at 400 °C for 40 h. After long-term test, the 1, 2-DCE conversion decreased from 89% to 74 %. It is speculated that the accumulation of chlorine over surface caused this deactivation in activity. In general, the investigated sample of γ-MnO_2 exhibited certain stability during activity test.

S9. Blank experiment

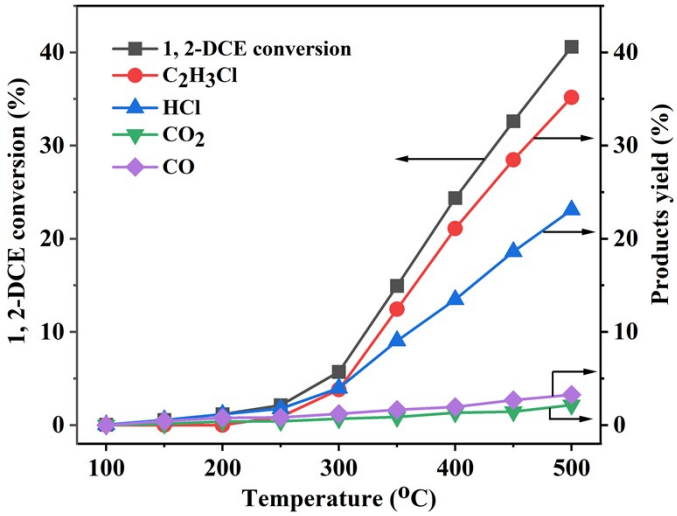

Figure S5. The blank experiment tested for decomposition 1, 2-DCE without catalysts.

A blank experiment in the absence of catalyst under the same experimental atmosphere for 1, 2-DCE oxidation was also conducted (Figure S5). The conversion of 1, 2-DCE was 40% at 500 °C with C_2H_3Cl as the main product, whose yield increased with temperature and reached 35% at 500 °C. In addition, the HCl and CO_2 yield were 23% and 2.15%, respectively. Therefore, it is necessary to further eliminate C_2H_3Cl using a suitable catalyst as well as improve the HCl and CO_2 yields..

References

[S1] T. Bjorkman. CIF_2Cell: Generating geometries for electronic structure programs. Computer Physics Communications, 2011, 182 (5) : 1183-1186.

[S2] Y. Pei. Mechanical properties of graphdiyne sheet. Physical Review B: Condensed Matter, 2012, 407 (22) : 4436-4439.

[S3] J. P. Perdew, K. Burke, M. Ernzerhof. Generalized gradient approximation made simple. Physical Review Letters, 1996, 77 (18) : 3865-3868.

[S4] J. P. Perdew, Y. Wang. Accurate and simple analytic representation of the electron-gas correlation energy. Physical Review B: Condensed Matter, 1992, 45 (23) : 13244-13249.